Combination of Aileron and Flap Deflection for Minimum Induced Drag Roll Control

By Winfried M. Feifel, Boeing Marine Systems Division

Presented at the XVIth OSTIV Congress, Chateauroux, France, July 1978

1. SUMMARY

Induced drag has a significant impact on the performance of flight vehicles. If a considerable amount of the airborne time is spent in maneuvering flight, optimization of vehicle performance requires the minimization of drag associated with maneuvering. In this study only the increment in induced drag due to aircraft lateral control and lateral control induced adverse yaw is analyzed theoretically, using an induced drag minimizing three-dimensional potential flow computer program. The effects of varying single-segment aileron span and employment of double-segment ailerons with an optimum combination of inboard and outboard control surface deflection angles and the merits of differentiating the upward and downward aileron deflection angles are investigated. The influence of wing induced sidewash onto the vertical tail induced drag due to aircraft yaw trim sideforces is accounted for. The optimum size of conventional ailerons is found to be in the order of 70% semispan. Double-segment aileron systems exhibit a slightly lower induced drag increment. They also require smaller control deflection angles and, therefore, should yield additional reductions in viscous profile drag.

2. INTRODUCTION

The straight line glide performance of sailplanes has been improved dramatically over the past 15 years and seems now to come close to the theoretical limits, at least in the case of standard class gliders. However, during a typical cross-country flight, a glider spends a significant fraction of the airborne time in maneuvering or circling flight. Therefore, high cross-country traveling speed is the product of both the glide performance and the thermalling capabilities of the sailplane. The process of finding and centering thermals involves a good deal of maneuvering flight. In the quest for maximum glide performance and a low rate of sink during circling flight, many designers have neglected to consider the airplane handling characteristics and the drag due to control deflections during transient flight conditions. Thus, further performance improvements can be expected from an optimization of sailplane maneuvering characteristics. Many gliders equipped with flaps droop the ailerons in conjunction with the flaps for slow flight. Immediately the question arises whether there are merits in utilizing differential deflections of the flaps to aid in the lateral control of the aircraft.

This paper theoretically analyzes for an elliptic wing of the aspect ratio 20 –parameters representative for sailplane configurations– the induced drag increments in potential flow due to lateral control. The following points will be addressed:

- Effect of the ratio of aileron span to wing span for conventional single-aileron systems
- Effect of using aileron and inboard flap deflections for roll control
- Effect of differentiation of the amount of upward and downward flap travel on induced drag and the induced adverse yawing moment
- Drag due to vertical tail side load for yaw trim

3. ANALYSIS

Viscous effects were not included in this analysis, although the profile drag increments due to control deflection angles may be as large or even larger than the induced drag increment. The potential flow analyses were performed with a three-dimensional vortex lattice computer program. This program is capable of minimizing the induced drag of an arbitrary aerodynamic configuration while satisfying a set of constraint conditions such as prescribed lift, sideforce, or moments. At the same time, the program determines the wing angle of attack and control deflections required to achieve these optimum conditions. Details on this method are described in reference 1.

For the potential flow analysis, the following assumptions were made:

- Quasi-steady-state aerodynamics can be applied
- No rollup of the trailing vorticity shed by lifting surfaces
- Only one degree of freedom of motion (roll)
- Rigid airplane

3.1 General Remarks on the Aerodynamics of Roll Control

Figure 1 explains the coordinate system and most of the symbols used in the present analysis. The rolling moment and yawing moment coefficients (C_{M_X},

C_{M_Z}) as well as the roll- and yaw-damping coefficients in this report have been nondimensionalized with the aircraft span (b) rather than the half span (s) used in most of the literature.

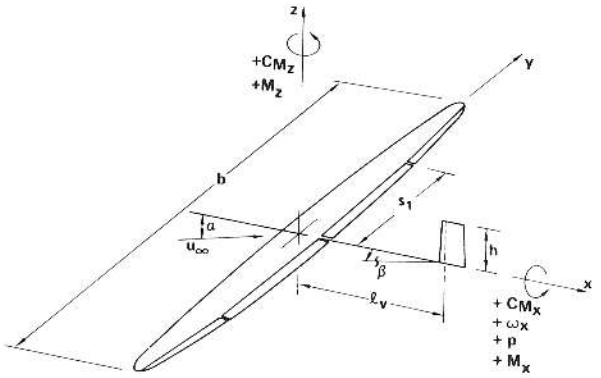

Fig. 1. Coordinate System and Nomenclature

The forces and moments acting on an aircraft are most easily explained by considering the two limiting cases.

At the beginning of the maneuver, there is only the static rolling moment ($C_{M_{XO}}$) acting on the wing, but the rate of roll (ω_X) is zero. This condition is depicted in figure 2. The trailing vortices shed by the wing antisymmetric load distribution are seen to induce upwash (W) at the left side of the wing and downwash at the right side. In addition, sidewash (V) is induced, which points away from the direction of the intended turn.

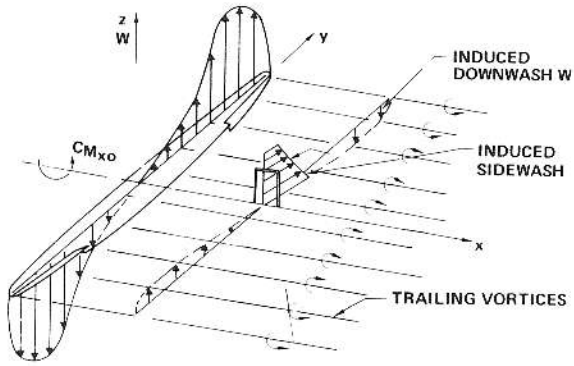

Fig. 2. Rolling Moment $C_{M_{XO}}$ and Induced Velocities Due to Aileron Deflection

Figure 3 shows the load distribution for the other limiting case, where the ailerons are not deflected but the wing is rotating at the rate ω_X. The load distribution generated by the rotation of the wing creates a rolling moment ($-C_{M_X}$), which counteracts the rolling motion. This rolling moment is referred to as roll damping moment ($\partial C_{M_X}/\partial\omega_X$) and depends only on the shape of the wing planform. The velocities induced by the rolling motion are seen to have two different sources: the rigid body motion due to ω_X and the velocities induced by the roll-generated spanwise load distribution.

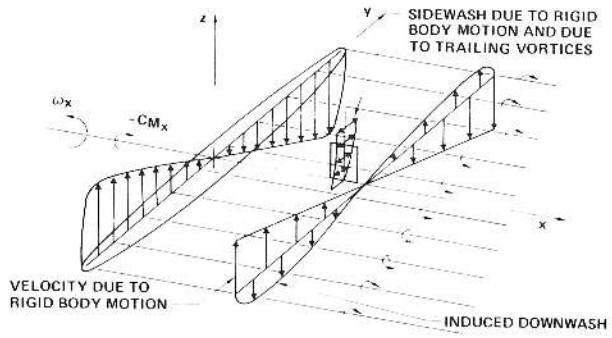

Fig. 3. Roll Damping Moment C_{M_X} Due to Wing Roll Rate ω_X

A steady-state rate of roll is obtained when the static rolling moment ($C_{M_{XO}}$) of figure 2 is canceled by the roll damping moment in figure 3. In both figures 2 and 3, the left side of the wing is seen to predominantly experience induced upwash velocities while the right side experiences downwash. This condition is sketched in figure 4. The change in the direction of the relative wind causes the lift vector on the left wing to be tilted forward and backward on the right wing. The resulting thrust drag couple causes the induced (adverse) yawing moment due to roll. For a given roll rate, the adverse yawing moment is directly proportional to the wing lift coefficient.

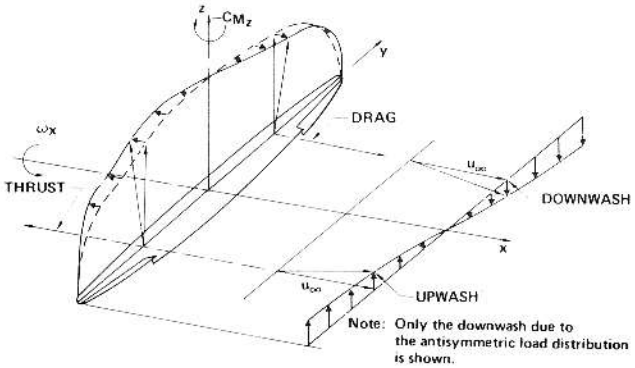

Fig. 4. Roll Induced Yawing Moment

3.2 Minimum Induced Drag Antisymmetric Load Distribution

The spanwise load distribution that yields the minimum amount of induced drag for a given wing static rolling moment ($C_{M_{XO}}$) is shown in figure 5. For an elliptic wing, this implies a linear variation of the section local lift coefficient (C_ℓ) between the two wingtips. Such a load distribution is achieved by a linear

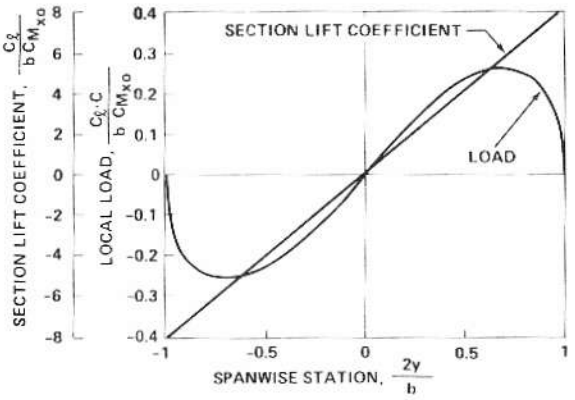

Fig. 5. Minimum Induced Drag Load Distribution on an Elliptic Wing for a Given Rolling Moment (Linear Wing Twist Distribution)

twist distribution from the wingroot to the wingtip.

The load distribution due to roll damping is shown in figure 6. The curves of figures 5 and 6 are similar, except for a scale factor. This yields the obvious result that the incremental induced drag of an elliptic wing in steady-state roll ($C_{M_X} = 0$) is a minimum (in fact 0) when it has a linear twist distribution. Then the load distributions due to the static rolling moment ($C_{M_{XO}}$) and due to roll damping cancel each other, and only the basic elliptic load distribution of steady-state level flight remains.

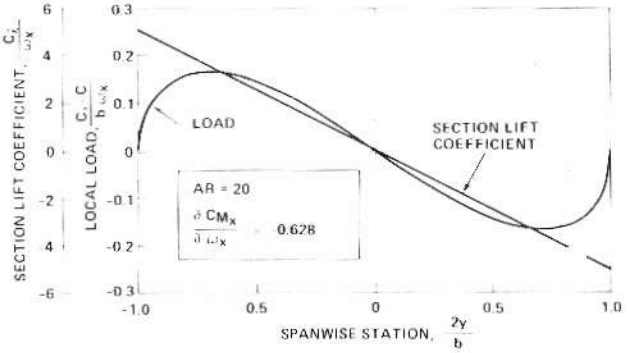

Fig. 6. Load Distribution Due to Roll on an Elliptic Wing (Roll Damping)

Figure 7 shows the induced drag increment due to roll as a function of the wing rolling moment. During the steady-state condition ($C_{M_X} = 0$), the drag increment is seen to be zero and independent of the roll rate. The drag increment for the elliptic wing of aspect ratio 20 is approximated by the expression

$$\Delta C_{Di} = 2\,C_{M_X}\,\omega_X + 0.515\,C_{M_X}^2 \qquad (1)$$

It is interesting to note that there is an optimum way to reduce the rate of roll and that, in fact, some forward thrust can be obtained. Differentiating equation (1) with respect to C_{M_X} indicates that the optimum roll deceleration is achieved when at every instant the counteracting rolling moment is of the magnitude $C_{M_X} = 1.94\,\omega_X$.

While linear wing warping is not a practical means of roll control for present aircraft construction techniques, this optimum condition can be used as a yardstick to compare the merits of other more practical solutions for aircraft roll control. In the subsequent analyses, it will be assumed that the control surfaces are rigid and that the control surface chord length is a constant fraction of the local wing chord length.

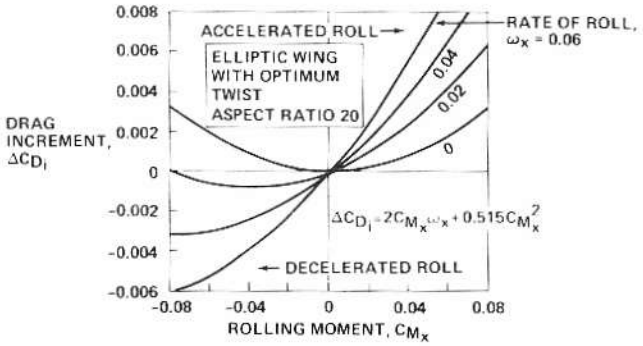

Fig. 7. Induced Drag Increment Due to Roll Rate ω_X and Rolling Moment C_{M_X} for an Elliptic Wing With Optimum (Linear) Twist Distribution

3.3 Roll Control With Outboard Ailerons

Most aircraft are equipped with ailerons extending from a spanwise station (s_1) to the wingtip. Figure 8 shows, for a given static rolling moment ($C_{M_{XO}}$), the antisymmetric spanwise load distributions for such aileron arrangements. For comparison the ideal load distribution for a twisted elliptic wing has been added. Figure 9 shows the spanwise variation of the section lift coefficient for the same conditions. The maximum incremental section lift coefficient required for a given static rolling moment ($C_{M_{XO}}$) decreases rapidly with increasing span of the aileron.

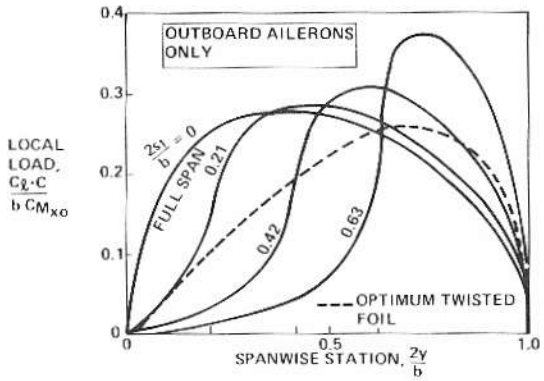

Fig. 8. Antisymmetric Load Distribution About an Elliptic Wing With Part-Span Ailerons of Constant Chord Ratio for a Prescribed Wing Rolling Moment

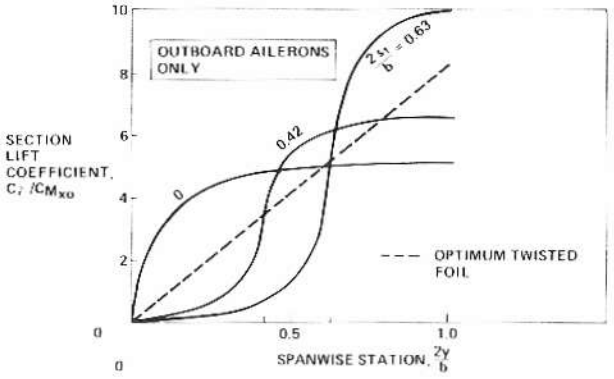

Fig. 9. Incremental Section Lift Coefficient for an Elliptic Wing With Part-Span Ailerons of Constant Chord Ratio for a Prescribed Wing Rolling Moment

Therefore, large-span ailerons should provide better control power at low speeds when the wing operates close to stall. In both figures 8 and 9, ailerons starting at approximately 30% wing semispan seem to yield conditions closest to the theoretically best linear twist distribution. This will be discussed further in the next paragraphs.

3.4 Roll Control With Aileron and Inboard Flap Deflection

An additional degree of freedom is introduced if both the ailerons and the inboard flaps can be deflected to create a prescribed static rolling moment. The condition that the induced drag due to the rolling moment must be a minimum yields the optimum deflection schedule for the inboard and outboard ailerons. The resulting optimum spanwise load distributions and local section lift coefficient variation are shown in figures 10 and 11. Compared to the single-aileron-only configurations, the two-segment aileron approximates much better the ideal optimum conditions; therefore, lower drag increments can be expected.

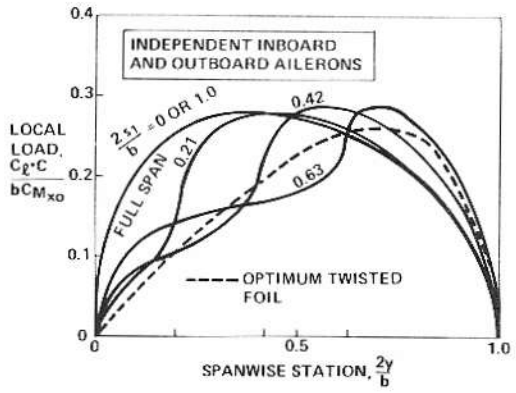

Fig. 10. Minimum Induced Drag Antisymmetric Load Distribution About an Elliptic Wing With Constant Chord Ratio Ailerons for a Prescribed Wing Rolling Moment

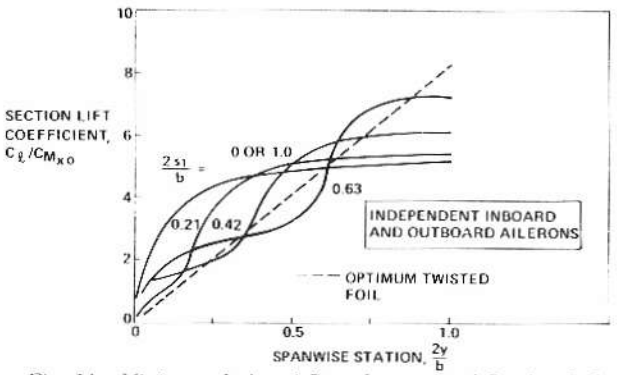

Fig. 11. Minimum Induced Drag Incremental Section Lift Coefficient for an Elliptic Wing With Constant Chord Ratio Ailerons at a Prescribed Wing Rolling Moment

3.5 Flap Deflection Angles Required

Rather than presenting the actual flap deflection angles required to achieve the load distributions described in the previous paragraph, the change in wing section angle of zero lift will be given. With the aid of figure 12, the angle of zero lift change can be translated into the equivalent flap deflection angle, depending on the flap chord to section chord ratio (C_f/C). Contrary to the viscous drag, the induced drag is independent of the flap chord ratio selected.

It should be noted that for minimum induced drag in the case of an elliptic wing, equally large positive and negative flap deflection angles are required. Viscous effects, however, in general limit the allowable downward aileron travel. The induced drag penalty associated with flap-up and flap-down travel differentiation will be discussed later in this paper. Section viscous drag increases rapidly at high flap angles, which therefore must be avoided. Figure 13 shows, for a given static rolling moment ($C_{M_{XO}}$), the required change in wing section angle of zero lift as a function of spanwise location (s_1) of the inboard end of the outboard ailerons. Compared to a full-span aileron ($s_1 = 0$), a typical single aileron starting at

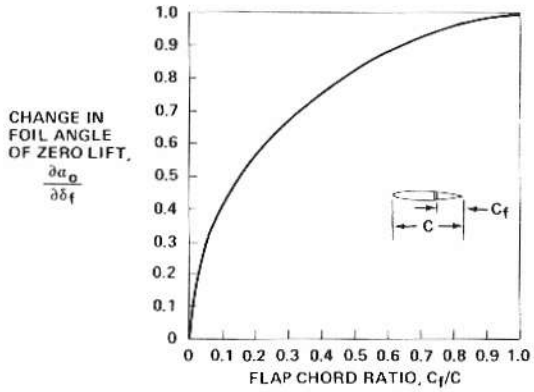

Fig. 12. Change in Foil Section Angle of Zero Lift as a Function of the Flap Chord Ratio (Thin Airfoil Theory)

$s_1 = 0.60$ requires nearly twice the deflection angle. In the case of a segmented aileron, the optimum deflections of the inboard flap panel are relatively small. The jump in deflection angle between the inboard and outboard aileron is nearly independent of the spanwise location of the breakpoint. Compared to the single aileron concept, there is a significant reduction in the outboard aileron deflections required. Therefore, independent of the induced drag characteristics, noticeable reductions in viscous drag due to control surface deflection can be expected from the use of segmented ailerons.

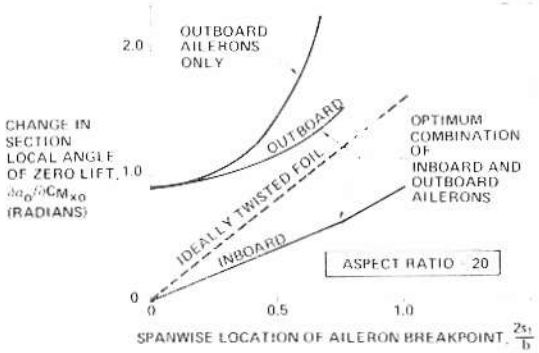

Fig. 13. Change in Aileron Section Angle of Zero Lift Required for Roll Control of an Elliptic Wing

3.6 Induced Drag Due to Lateral Control

The wing induced drag increment due to lateral control inputs is, in the case of an elliptic wing, independent of the wing lift coefficient. When the spanwise load distribution generating the static rolling moment ($C_{M_{XO}}$) has not been the result of a linear twist distribution, the load distribution due to roll damping will still cancel the rolling moment ($C_{M_{XO}}$) but once the steady-state rate of roll has been reached, there will remain a residual spanwise load distribution due to the control deflection. This load distribution causes induced drag that, for a given configuration, is proportional to the square of the roll rate (ω_X). The induced drag increment due to roll control is described by the equation

$$\Delta C_{Di} = K_1 C_{M_X} \omega_X + K_2 C_{M_X}^2 + K_3 \omega_X^2 \qquad (2)$$

Figure 14 presents the values for the constants K_1 through K_3 as a function of the spanwise location of the aileron breakpoint (s_1). The induced drag increment is seen to be a minimum when s_1 is located at approximately 30% span in the case of single aileron control, while in the case of double-segment ailerons the optimum is reached for $s_1 \approx 0.45$. There seems to be no striking drag difference between the optimum span single-element aileron and the double-segmented counterpart. However, the drag penalty for short-span single-segment ailerons, as they are commonly used in most aircraft, is more significant.

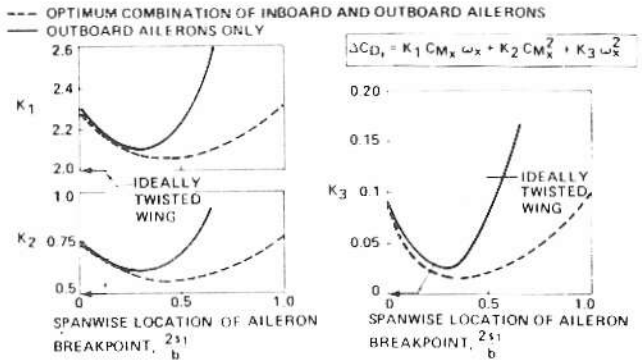

Fig. 14. Induced Drag Increment for an Elliptic Wing of the Aspect Ratio 20 Due to Lateral Control Inputs With Constant Chord Ratio Ailerons

3.7 Analysis of the Rolling Motion

The following analysis provides some insight into the relative significance of the various drag terms in equation (2). The time dependent rolling motion of an aircraft, neglecting effects of virtual mass, can be described by the following differential equation (ref. 2)

$$\underbrace{\frac{I_X}{0.5\rho u_\infty^2 bA} \cdot \frac{dp}{dt}}_{\text{roll acceleration inertia moment (=0 at steady roll)}} = \underbrace{C_{M_{XO}}}_{\text{static rolling moment}} + \underbrace{\frac{\partial C_{M_X}}{\partial \omega_X} \cdot \frac{b}{2u_\infty} p}_{\text{roll damping moment}} \qquad (3)$$

where

I_X = inertia of the aircraft about the roll axis [kg m^2]
ρ = density of the air [kg m^{-3}]
b = wing span [m]
A = wing area [m^2]
p = $2u_\infty \omega_X / b$ = aircraft rate of roll [sec^{-1}]
u_∞ = speed of the aircraft [m sec^{-1}]

Figure 15 presents a numerical solution of equation (3) for a typical standard class glider, assuming that a maximum nondimensional roll rate of $\omega_X = 0.07$, a value representative for many aircraft, can be attained. The ailerons were assumed to be deflected so that after 0.3 sec the maximum static rolling moment ($C_{M_{XO}} = 0.044$) was achieved. To stop the roll, the controls were assumed to be returned to the neutral position also within 0.3 sec. The static rolling moment was assumed to be generated by optimum linear wing twist or by differentially deflected ailerons ($s_1 = 0.63$), respectively. Data from the previ-

ous paragraphs were used to calculate the induced drag increment. During the roll acceleration time of approximately 0.8 sec, the ideally twisted wing is seen to experience an incremental induced drag, which is partly related to the work stored in the roll momentum of the aircraft. After the acceleration phase, a steady rate of roll is maintained with zero induced drag increment. During the deceleration phase, part of the energy stored in the rolling mass is recuperated in the form of negative induced drag.

The aircraft with part-span ailerons shows basically the same characteristics, but the drag levels are higher, and, most significantly, there is a constant amount of incremental induced drag during the time

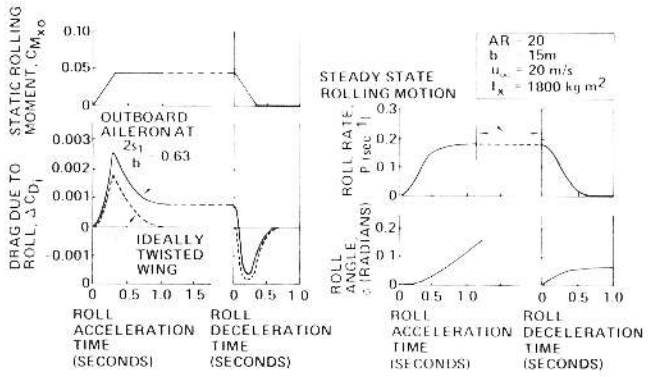

Fig. 15. Roll Characteristics of an Elliptic Wing Typical for a Standard Class Glider at Sea Level

period of steady roll. Assuming that the aircraft is going to change its lateral attitude by 90 degrees, about 80% of the maneuvering time is spent in steady-state roll, and the drag experienced during steady-state roll becomes the most significant factor.

3.8 Effect of Aileron Differentiation

Generally the downward travel of ailerons is smaller than the upward deflections. This differentiation of the deflection angles is necessary to avoid viscous flow separation at the wing half with downward deflected ailerons. Aileron differentiation also affects the roll induced adverse yawing on the wing. This roll-yaw coupling has a pronounced influence on the handling characteristics. The yawing moments are caused by spanwise variation of profile drag and induced drag. Only the induced drag related problems will be addressed in this paper.

3.8.1 Effect of Aileron Differentiation on Drag

If the basic wing lift distribution is elliptic, differentiation of the aileron deflections will always increase the incremental induced drag due to roll control. An upper limit of the induced drag penalty is obtained analyzing the case where only upward aileron deflections are allowed ($\delta_{down}/\delta_{up} = 0$). Figures 16 and 17 show the induced drag constants K_2 and K_3 for these limiting cases. The constant K_1 was not determined because it is significant only during the brief roll acceleration and deceleration period. There is a significant drag penalty for the unusually large aileron differentiation ratio of $\delta_{down}/\delta_{up} = 0$.

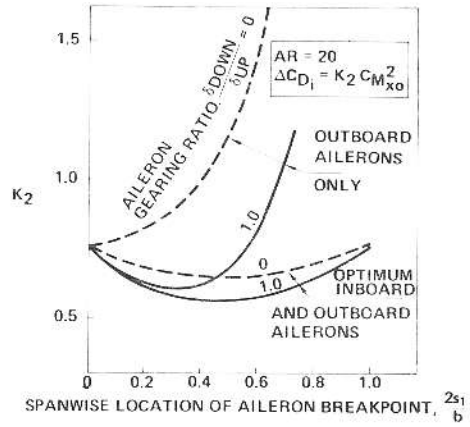

Fig. 16. Effect of Aileron Differentiation on Induced Drag of an Elliptic Wing at a Constant Static Rolling Moment

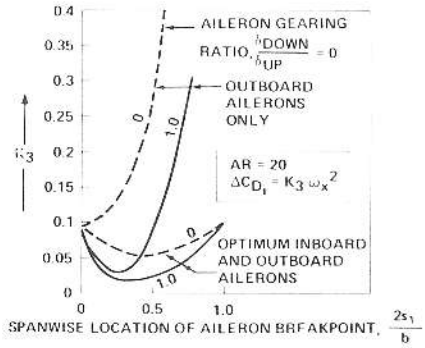

Fig. 17. Effect of Aileron Differentiation on Induced Drag of an Elliptic Wing at Steady Rate of Roll

Figure 18 shows the induced drag constants K_2 and K_3 as a function of the aileron differential gearing ratio. The drag penalty is seen to be small for gearing ratios $\delta_{down}/\delta_{up} > 0.5$. Differentiation of full-span

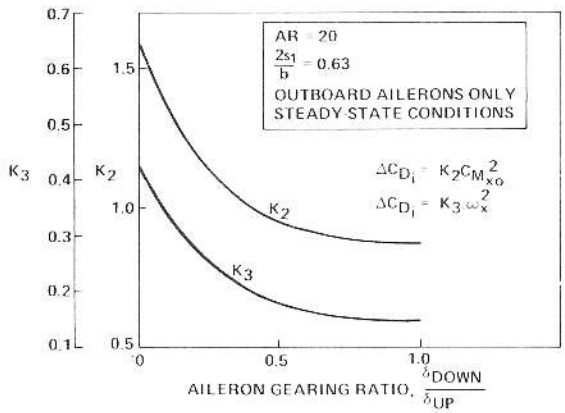

Fig. 18. Effect of Aileron Differentiation Gearing Ratio on the Induced Drag Due to Lateral Control of an Elliptic Wing

single-segment ailerons has no effect on the induced drag.

3.8.2 Effect of Aileron Differentiation on the Induced Yawing Moment

For an elliptic wing with symmetrically deflected ailerons, the lateral control introduces an induced yawing moment that is described by the expression

$$C_{M_Z} = (K_6\,\omega_X + K_7\,C_{M_X})\,C_L \qquad (4)$$

For a wing of aspect ratio 20, these constants are K_6 = -0.125 and K_7 = -0.048. The minus sign indicates that this yawing moment tries to move the downward rolling side of the wing forward opposite to the direction of the intended turn.

If the aileron differentiation ($\delta_{down}/\delta_{up} \neq 1$) is used, additional terms (ω_X^2, $C_{M_X}^2$, $C_{M_X}\,\omega_X$) must be introduced in equation (4). Only the terms related to ω_X^2 and $C_{M_X}^2$ have been calculated and are shown in figure 19 for $\delta_{down}/\delta_{up} = 0$ as a function of the spanwise location of the aileron breakpoint (s_1). Aileron differentiation is seen to create a positive roll induced yawing moment at lift coefficients up to

$$C_L \leq \frac{K_4\omega_X}{K_6} \quad \text{for } C_{M_X} = 0.$$

Aileron differentiation is more effective in the case of conventional aileron arrangements than for segmented aileron designs. The induced yawing moment of single-segment full-span ailerons is not affected by aileron differentiation. Figure 20 shows the variation of the terms K_4 and K_5 as a function of the gearing ratio for a typical conventional aileron.

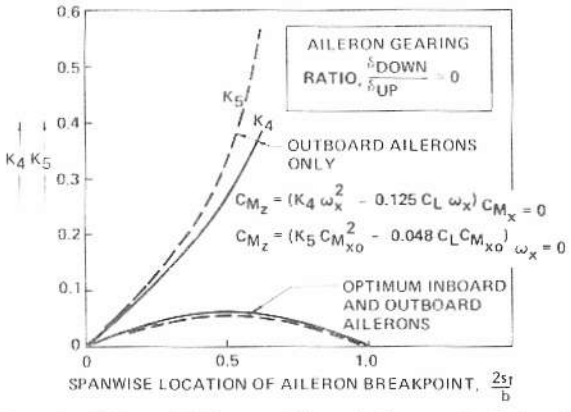

Fig. 19. Effect of Aileron Differentiation on the Induced Yawing Moment of an Elliptic Wing of Aspect Ratio 20

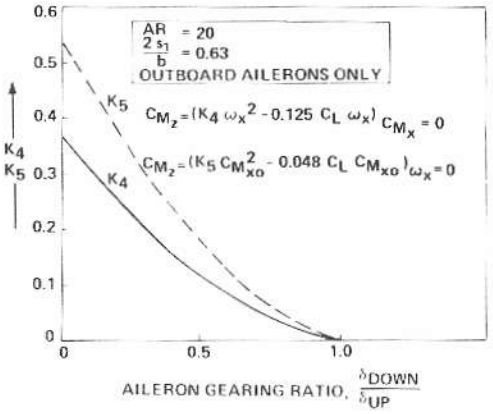

Fig. 20. Effect of Aileron Differentiation Gearing Ratio on the Induced Yawing Moment of an Elliptic Wing

3.9 Lateral Control Induced Sidewash

The trailing vortex system shed by the antisymmetric load distribution on the wing induces a sidewash (V), which in turn influences the forces acting at the vertical tail of the aircraft. Figure 21 shows the sidewash induced 0.3 span downstream of a wing with ailerons deflected to generate a static rolling moment ($C_{M_{XO}}$). In addition, the only wing planform

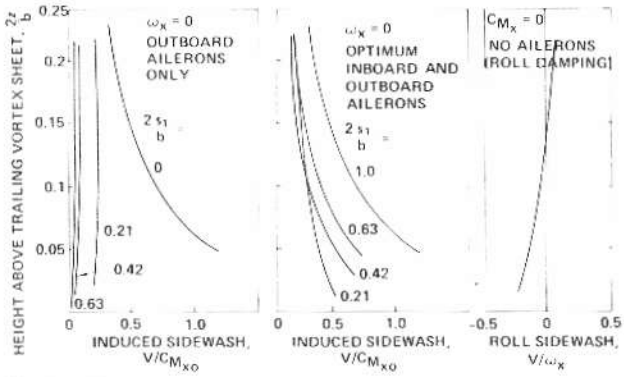

Fig. 21. Sidewash Induced 0.3 Span Downstream of an Elliptic Wing Due to Lateral Control

dependent sidewash resulting from the roll rate (ω_X) and its corresponding roll damping load distribution are shown. Any intermediate condition can be obtained from a linear superposition of these two limiting cases. The sidewash is seen to be especially strong in the case of full-span ailerons or segmented ailerons. The sidewash creates a sideforce at the vertical tail. This sideforce tends to counteract the adverse induced yawing moment if the vertical tail is located above the trailing vortex sheet, thus improving the aircraft handling characteristics.

If the vertical tail is located above the trailing vortex sheet, the sidewash can also reduce the induced drag acting on the vertical tail due to the sideforce required for yaw trim, as is explained in fig-

ure 22. The vertical tail lift vector is rotated forward by the sidewash angle (ϵ) creating forward thrust. This beneficial effect is more pronounced in the case of segmented and full-span ailerons.

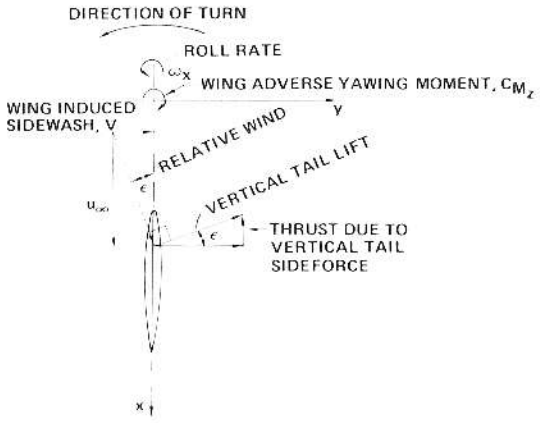

Fig. 22. Reduction of Vertical Tail Induced Drag Due to Sidewash Induced by the Wing

3.10 Analysis of Aircraft in Steady-State Rate of Roll

A typical standard class glider configuration with three different aileron arrangements has been analyzed at the steady-state rate of roll $\omega_X = 0.07$. The airplane was trimmed in yaw by an appropriate sideforce acting at the vertical tail. The aileron up and down deflection was differentiated at the rate $\delta_{down}/\delta_{up} = 0.5$. Figure 23 shows the result of this study. There is an increase in induced drag due to roll for all three aileron arrangements investigated. The drag penalty is the largest for the conventional part-span aileron. The induced drag increment for an optimized segmented aileron configuration is only slightly less than for a single-segment full-span aileron. There can be a significant additional savings in viscous drag since the average amount of control deflection is significantly less (see fig. 14) for the same control effectiveness in the case of the double-segment aileron arrangement.

The rudder deflection angles for yaw trim are the highest for the conventional part-span aileron. The segmented aileron requires less rudder movement and, therefore, can be expected to provide improved aircraft handling characteristics.

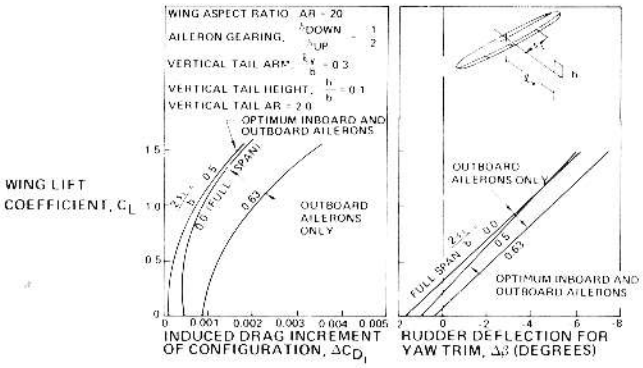

Fig. 23. Rudder Deflection for Yaw Trim and Induced Drag of a Configuration With an Elliptic Wing at a Steady Rate of Roll $\omega_X = 0.07$

4. CONCLUSIONS

There is a significant increase in induced drag during the execution of lateral control maneuvers, unless lateral control is achieved by theoretically best linear wing warping. The amount of additional induced drag depends on the details of the aileron design and varies proportionally to the square of the nondimensional roll rate.

The optimum size of conventional single-segment ailerons is in the order of 70% wing semispan, much larger than presently used for gliders. The aileron deflection angles required to achieve a given roll rate decrease rapidly with the span of the ailerons. Correspondingly, the increments in local section lift coefficient for roll control are reduced, which should result in better handling characteristics at low-speed operating conditions. Smaller aileron deflection angles can also be expected to reduce the profile drag increment due to viscous effects.

Full-span, double-segment ailerons with the optimum breakpoint located at approximately 50% semispan offer a slight reduction in induced drag over an optimum single-element aileron system. The main advantage of the double-segment aileron arrangement is that large deflection angles are applied only over the fraction of the wing where they are aerodynamically most effective. Viscous drag is saved by limiting the deflections of the inboard aileron, which affects a large fraction of the wing area.

Aileron differentiation is a powerful means to reduce the adverse induced yawing moment of short-span single-segment aileron configurations. It has little effect on the induced yawing moment of double-segment aileron arrangements and no effect on full-span single-element ailerons. The induced drag penalty is small for commonly used aileron differential deflection ratios.

The induced drag due to the sideforce required on the vertical tail to compensate for the induced wing yawing moment should not be neglected. The vertical tail drag is reduced by the sidewash induced by the trailing vortices. The double-segment aileron concept requires the least amount of rudder deflection to compensate for induced yaw and is therefore expected to give best aircraft handling characteristics.

5. NOMENCLATURE

A	wing area [m^2]
$AR = b^2/A$	wing aspect ratio
b	wing span [m]
C	wing section chord length [m]
C_{D_i}	induced drag coefficient
C_f	flap chord length [m]
C_L	wing lift coefficient
C_ℓ	section lift coefficient
$C_{M_X} = M_X/qbA$	wing rolling moment coefficient at roll rate ω_X
$C_{M_{XO}} = M_{XO}/qbA$	wing rolling moment coefficient at zero rate of roll
$C_{M_Z} = M_Z/qbA$	yawing moment coefficient
h	vertical tail height [m]
I_X	moment of inertia about x-axis [kg m^2]
K_1, K_2, K_3	coefficients in induced drag equation
K_4, K_5	constants describing the yawing moment change due to differential aileron deflections
$K_6 = \frac{1}{C_L}\left(\frac{\partial C_{M_Z}}{\partial \omega_X}\right)_{C_{M_X}=0}$	roll induced yaw coefficient
$K_7 = \frac{1}{C_L}\left(\frac{\partial C_{M_Z}}{\partial C_{M_X}}\right)_{\omega_X=0}$	rolling moment induced yaw coefficient
ℓ_v	vertical tail moment arm [m]
M_X	rolling moment at rate of roll ω_X [mN]
M_{XO}	rolling moment at zero roll rate [mN]
M_Z	yawing moment [mN]
p	roll rate [1/sec]
$q = \frac{1}{2}\rho u_\infty^2$	dynamic pressure [N/m^2]
s	wing half span [m]
s_1	distance from x-axis to start of outboard aileron [m]
t	time [sec]
u_∞	freestream velocity [m/s]
V	induced sidewash velocity [m/s]
W	induced downwash velocity [m/s]
a_o	section angle of zero lift
β	rudder deflection angle
ΔC_{Di}	induced drag increment due to lateral control
δ_{down}	aileron downward deflection angle
δ_f	flap deflection angle
δ_{up}	aileron upward deflection angle
ϵ	wing induced sidewash angle
ρ	air density [kg/m^3]
ϕ	aircraft roll angle
$\omega_X = pb/2u_\infty$	nondimensional roll rate

6. REFERENCES

1. Feifel, W. M., "Optimization and Design of Three-Dimensional Aerodynamic Configurations of Arbitrary Shape by a Vortex Lattice Method," *Vortex Lattice Utilization*, NASA SP-405, May 1976.
2. Perkins, C. D., Hage, R. E., *Airplane Performance Stability and Control*, John Wiley & Sons, Inc., New York, 1967.